Available online at www.sciencedirect.com
SCIENCE DIRECT
Surface & Coatings Technology 198 (2005) 68–73
SURFACE & COATINGS TECHNOLOGY
www.elsevier.com/locate/surfcoat

Growth of AlN films on Si (100) and Si (111) substrates by reactive magnetron sputtering

J.X. Zhang[a,*], H. Cheng[a], Y.Z. Chen[a], A. Uddin[a], Shu Yuan[a], S.J. Geng[b], S. Zhang[b]

[a]*School of Materials Engineering, Nanyang Technological University, Singapore 639798, Singapore*
[b]*School of Mechanical and Production Engineering, Nanyang Technological University, Singapore 639798, Singapore*

Available online 14 November 2004

Abstract

GaN has shown great potential for high-power high-frequency electronic devices and short-wavelength optical devices. To integrate GaN-based optoelectronic devices with Si-based electronic devices and reduce the cost, it is desirable to grow epitaxial GaN thin films and device structures on the Si substrate. However, a proper buffer layer is essential for epitaxial growth of GaN films on Si substrate due to large mismatch between them in the area of lattice constant, thermal expansion coefficient and chemistry feature. In the present work, the growth of AlN buffer layer was studied. Wurtzite aluminum nitride thin films were grown on Si (111) and Si (100) substrates using reactive sputtering deposition under different discharge powers. X-ray diffraction (XRD) patterns showed that full width at half maximum (FWHM) of AlN (0002) peak grown on Si (111) substrates was smaller than that grown on Si (100) substrates. Vibrational characterization by Fourier transform infrared spectroscopy (FTIR) revealed that the stress in the AlN films deposited on Si (111) substrates was also smaller than that deposited on Si (100) substrates. For Si (100) substrates, the large lattice mismatch between AlN (0001) and Si (100) is a main contribution to the large strain in the formed films. For Si (111) substrates, the strain in the films deposited on Si (111) largely depends on the discharge power in sputtering, and the strain due to defects and thermal mismatch contributes largely to the residual strain in the deposited films.
© 2004 Elsevier B.V. All rights reserved.

PACS: 81.15.C; 78.66.F
Keywords: Reactive sputtering; Silicon; Aluminum nitride; Stress; X-ray diffraction

1. Introduction

GaN has become one of the most important semiconductors. This is because blue and ultraviolet (UV) light emitting devices as well as high-temperature and high-frequency high-power electronic devices can be made of GaN-based structures [1]. Due to lack of a natural substrate, most GaN devices are made from multiple epitaxial layers grown on either sapphire or SiC. Sapphire and especially SiC are expensive and hard to process and thus introduce difficulties in device fabrication and cost. On the other hand, large, up to 12 in. diameter, and high-quality silicon wafers are readily available at relatively low cost. GaN electronic and optoelectronic devices on Si substrates are thus highly desirable and have the potential to be integrated with well-developed silicon microelectronic circuits [2]. However, it is still not commonly known how to realize high-quality epitaxial GaN layers on silicon. One route for this is to cover the Si substrate by AlN, which serves as a substrate for further GaN growth.

In general, the growth of epitaxial GaN layers on disparate substrates requires a critical buffer layer, and, in most cases, this layer [3–5] is AlN. This is a wide band gap (6.2 eV) III–V compound with high values on thermal conductivity, chemical and thermal stability, refractive index and breakdown dielectric strength. With these properties, the thermodynamically stable wurtzite AlN films are, not only good buffer layer materials for GaN growth, but also promising materials for applications in other microelectronic and optoelectronic devices [6,7]. There is some work concerning deposition of AlN buffer layers on sapphire or SiC substrates

* Corresponding author. Tel.: +65 6790 6161.
E-mail address: jxzhang@ntu.edu.sg (J.X. Zhang).

0257-8972/$ - see front matter © 2004 Elsevier B.V. All rights reserved.
doi:10.1016/j.surfcoat.2004.10.075

[3–5,8,9]. Less work has been devoted to the deposition of AlN to be used as a buffer layer on Si substrate for further GaN growth. Studies have been made by MBE or metal-organic vapor phase epitaxy (MOVPE) [10–12]. There are also other methods. Recently, Paskova et al. deposited high-temperature reactively sputtered AlN layers on sapphire and then grew a GaN film using hydride vapor phase epitaxy (HVPE) [13]. They found that the sputtered AlN buffer layers are effective in suppressing defect formation and reducing residual compressive stress in the GaN films. Wan et al. [14] grew hexagonal GaN films on Si (100) substrates by employing two-step buffer layer. A sputtered AlN buffer layer was followed by another high-temperature MOVPE grown AlN buffer layer. This approach with double buffer layers could achieve a shiny GaN surface and also eliminate cracking of the GaN layers up to their thickness of 2 μm. Since sputtering is an efficient and inexpensive method, it is challenging to find ways to grow high-quality AlN buffer layers for further GaN growth directly on Si.

The stress in the buffer layer is crucial for the quality of the GaN layer [15–17]. It is important to investigate the development of the strain or stress in the sputtered AlN film under different deposition conditions. In this work, we report the deposition of good quality AlN thin layer on Si (100) and Si (111) substrates by reactive sputtering under high vacuum. As GaN devices are usually made from hexagonal GaN epitaxial layers, Si (111) can provide the hexagonal template for AlN deposition. Si (100) is widely used in ultralarge-scale-integrated circuits as it has much fewer interface defects than Si (111). Therefore, we also compare the AlN characteristics deposited on both Si (100) and Si (111) wafers.

2. Experimental procedure

The RF magnetron sputtering system has a chamber with a water-cooled target disk of 120 mm diameter. The purity of the aluminum target used in the investigation is 99.999%. Prior to loading silicon substrates into the sputter chamber, the silicon substrates were cleaned in a solution of H_2O/HCl/H_2O_2 (6:1:1 by volume) at 70 °C and a solution of H_2O/H_2O_2/NH_4OH (5:1:1 by volume) at 70 °C and then dipped into a dilute solution of 5% HF to remove the surface oxide if any. After such cleaning, the substrates were rinsed in deionized water and blow-dried in N_2. The base vacuum of the deposition system was stabilized at approximately 2.8×10^{-7} Torr. Once the desired background pressure was reached, a gas mixture of N_2 and Ar was introduced into in the chamber. The target was presputtered for 10–20 min to clean and equilibrate the target surface prior to film deposition. The sputtering was processing for 1 h in the discharge power from 200 to 500 W. The substrate temperature was fixed at 350 °C, and the distance from the substrate to the target was kept constant at approximately 8 cm. During the deposition, pressure in the chamber was around 6 mTorr. The deposited film thickness is around 200–260 nm.

The crystal structures of AlN thin films were characterized by X-ray diffraction (XRD, Simens D5005). The crystallite sizes of AlN films and the film thickness were determined by field emission scanning electron microscopy (FESEM; JEOL JSM-6340F). Fourier transform infrared spectroscopy (FTIR; Perkin-Elmer S2000) was used to identify the chemical composition and structure of the films. The microstructure and defects of the films were observed by transmission electron microscopy (TEM; JEM 2010).

3. Results and discussion

The crystal structures of the AlN films were investigated by XRD employing Cu Kα(1.5406 Å) radiation. Fig. 1 shows the X-ray diffraction spectra of the samples prepared at discharge powers of 200, 300, 400 and 500 W. On the Si (100) substrates, the deposited AlN films present features at

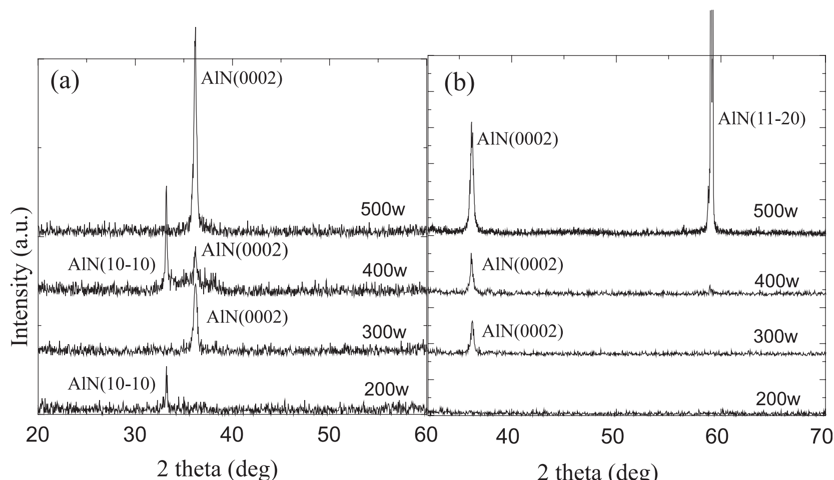

Fig. 1. X-ray spectra obtained from AlN films deposited at discharge powers of 200, 300, 400 and 500 W on (a) Si (100) substrates and (b) Si (111) substrates.

around 33° and 36° corresponding to the (10–10) and (0002) planes of crystalline AlN (Fig. 1(a)). The films show (10–10) preferential orientations at a discharge power of 200 W, in comparison with mixed (0002) and (1000) orientation at a discharge power of 400 W. However, under discharge power of 300 and 500 W, the films show high *c* axis orientation. The alignment of the Si (100) peak with AlN (0002) indicates that the basal plane (0001) of AlN is parallel to the (100) plane of silicon substrate. When the Si (111) substrates are used, AlN films can exhibit features at around 36° and 59°, corresponding to the plane of (0002) and (11–20) of AlN (Fig. 1(b)). Under low discharge power, i.e., 200 W, the film has not presented preferred orientation. The film shows strong (0002) *c*-axis-preferred orientation when the power is increased to 300 W. However, the (11–20) orientation gradually increases to make the AlN film present mixed (0002) and (11–20) orientation with the power above 400 W.

The crystallographic orientation of the grains in the film is determined by the preferential growth of certain crystal planes over others. The mechanism of preferential orientation of AlN films can be explained by the crystalline lattice structure of AlN. As shown in Fig. 2, the hexagonal wurtzite structure of AlN has two kinds of Al–N bond named as B_1 and B_2 [18], where the bond energy of B_1 is relatively larger than that of B_2. In the AlN structure, the plane of (10–10) is composed of bond B_2, while the planes of (0002) and (11–20) consist of the bonds B_1 and B_2 together. Therefore, the energy required for sputtering particles to be deposited in the planes of (0002) and (11–20) are relatively larger. Under lower discharge power, the films present *a* axis orientation ((10–10) plane formation) or no preferred orientation. With increasing power, the growth of AlN films exhibits *c* axis orientation ((0002) plane formation) or mixed orientation ((0002) and (11–20)

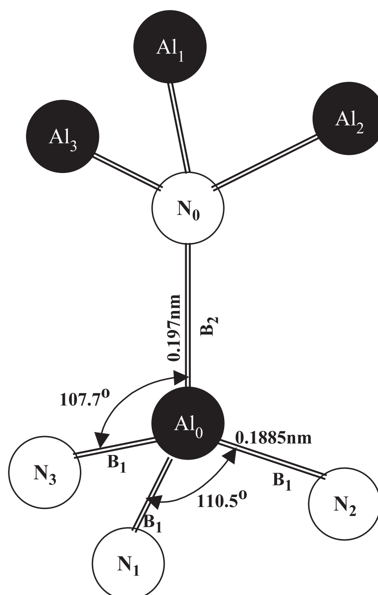

Fig. 2. The schematic diagram of wurtzite AlN structure from Ref. [17].

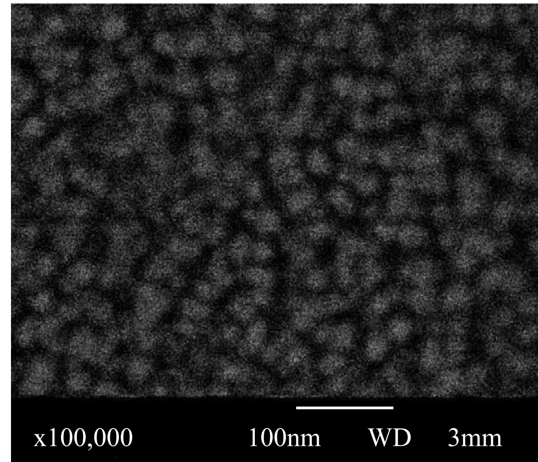

Fig. 3. Typical FESEM photograph of the AlN films grown on Si (100) substrate at a discharge power of 500 W.

planes). XRD results also indicate that the preferred orientation of AlN films on Si (111) substrates is more easily controlled than those on Si (100) substrates. It can be attributed to the more matched lattice template with hexagonal structures of AlN films provided by (111) plane of silicon, which will be further elaborated in the following.

The XRD spectra can also present that the full width at half maximum (FWHM) of the peak (0002) changes with discharge powers and the orientations of the substrates. When (100) silicon was used as substrates, the FWHM is 0.434° for discharge power of 300 W, while it decreased to 0.342° at 400 W and 0.327° at 500 W. Comparatively, on Si (111) substrates, the FWHM of the (0002) peak does not change obviously with discharge power, and all of them shows small value of around 0.3°. Although the AlN films exhibit only (0002) preferred orientation on both Si (100) and Si (111) substrates under the same deposition condition, i.e., 300 W, the FWHM of the (0002) peak for the films on Si (111) is much smaller than that on Si (100). The difference in the FWHM of XRD peaks can be investigated by the grain sizes and the stress distribution. As we know, the crystallite size and the nonuniform strain field with local lattice parameter change due to the interface, and/or dislocation contributes to the width broadening of a diffraction peak, as expressed by the following equation [19]:

$$\beta = k\lambda/(d\cos\theta) + \varepsilon\tan\theta \quad (1)$$

where λ is the wavelength of the X-rays, θ is the diffraction angle, ε is the strain, d is the crystallite size, k is a constant (0.94 for Lorentzian line profiles and small crystals of uniform size), and β is the corrected full width at half maximum of the peak. The crystallite sizes are identified by the FESEM photographs, and Fig. 3 shows typical FESEM photos sputtered at 500 W. The crystallite sizes of the AlN films on the Si (100) substrates are 26, 25, 35 and 40 nm under discharge powers of 200, 300, 400 and 500 W, respectively. As for the Si (111)

substrates, the crystallite sizes are 28, 30, 34 and 42 nm, respectively. Generally, the mobility of the reactive species is increased with increasing sputtering power. Thus, the nucleation and growth rate are increased accordingly. As a result, the crystal size increases with RF power. However, the crystal sizes increase slowly at low sputtering power. Therefore, the crystal sizes did not change too much at 200 and 300 W for Si (100) substrates. Within the error of measurement and system, the results are reasonable. By substituting the measured crystallite sizes into Eq. (1), the strain in the films can be determined ($\varepsilon=\beta/\tan\theta-k\lambda/(d\sin\theta)$). Fig. 4 shows the strains in the AlN films with discharge power for both Si (100) and Si (111) substrates. It can be seen that the strain in the deposited films increases with higher discharge power irrespectively of the orientation of silicon substrates. The augmentation of the stress is related closely to the increase of particle collision with the increasing of power. It can also be observed that the stress between the deposited AlN film and substrate Si (111) is decreased compared to Si (100) substrate. The strain of the AlN film on Si (100) substrates does not change too much with discharge power, while the strain of the AlN films on Si (111) substrates obviously depends on discharge power.

FTIR is an effective technique to investigate characteristic vibration modes of the lattice. Fig. 5 presents the spectra of the films deposited at discharge power of 200, 300, 400 and 500 W on Si (100) and Si (111) substrates, respectively. These spectra were obtained by subtracting the background of the corresponding silicon substrates. It was reported that crystalline AlN exhibits the characteristic modes at ~611, ~670, ~890 and ~912 cm^{-1} arising from A_1(TO), E_1(TO), A_1(LO) and E_1(LO) vibration modes, respectively, which are IR active [20–22]. Accordingly, the strong peak near 680 cm^{-1} in Fig. 5 can be attributed to the contribution from the phonon modes of E_1(TO) [21,22]. Due to the residual stress in the AlN film induced from sputtering process, the FTIR peaks shift from their characteristic position [20–22]. The peak position was determined by second derivative of the FTIR curve. For Si (100) substrates, the peak positions shifted to 681, 684, 686 and 691 cm^{-1} under the power of 200, 300, 400 and 500 W, respectively. The peak shift for Si (111) substrates is smaller under the same deposition conditions, which is 677, 678, 679 and 688 cm^{-1} for the deposition power of 200, 300, 400 and 500 W, respectively. According to the literatures [23], the E_1(TO) peak position in the stress-free AlN film is 673 cm^{-1}, and the residual stress in the deposited films can lead to a higher wave number shifting in FTIR peaks with a coefficient of 8 cm^{-1}/GPa. Accordingly, the residual stress for the Si (100) substrates is 1, 1.4, 1.6 and 2.3 GPa, respectively, while the stress for the Si (111) substrates is 0.5, 0.6, 0.7 and 1.9 GPa, respectivley. With the increase of discharge power, the stress in the film increases irrespectively of the orientation of silicon substrates. It can also be observed that the film stress deposited on Si (111) substrates is decreased compared to Si (100) substrates. These findings about the influence of power on the stress of the films on Si (111) substrates and the effect of substrate orientation on the stress of the films agree well with the XRD results discussed earlier.

The presence of the residual stress in the sputtered films arises from three factors: (1) intrinsic stresses due to defects; (2) lattice or domain mismatch stresses and (3) thermal residual stress due to different coefficient of thermal expansion between substrates and the deposited films. The defects in the deposited AlN films are complex such as vacancies, dislocations, grain boundaries and impurities. Fig. 6 shows the cross-sectional TEM picture of AlN film on Si (100). The morphology of the film on Si

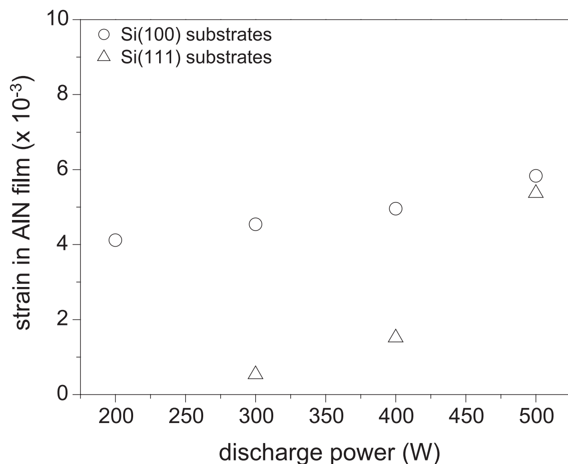

Fig. 4. Sputtering-power-dependent strain in the deposited AlN films on silicon substrates.

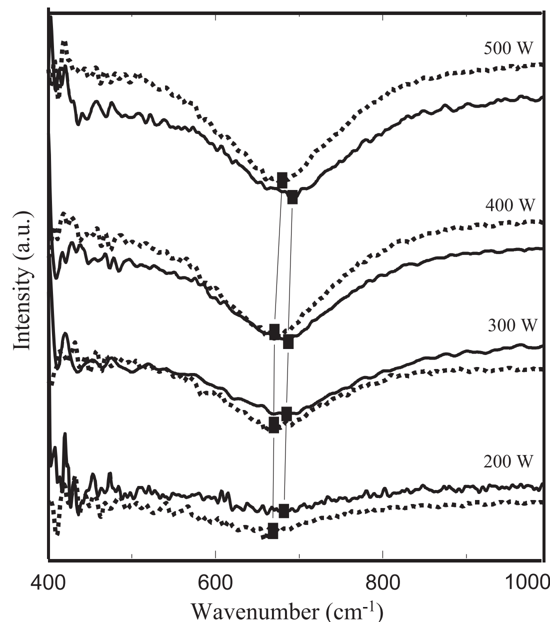

Fig. 5. FTIR transmittance spectra of AlN thin films deposited under different discharge power on Si (100) substrate (solid line) and Si (111) substrate (dotted line).

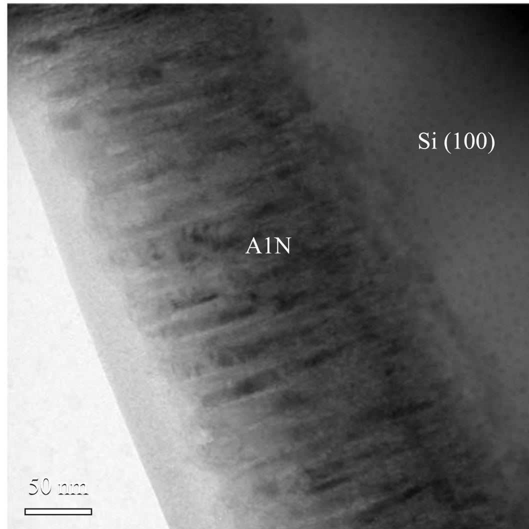

Fig. 6. The cross-sectional TEM picture of AlN film on Si (100) substrate.

(111) is similar. It can be clearly observed that the AlN layers are columnar structure consisting of slightly misoriented subgrains bounded by threading dislocations [24]. Due to the high affinity of Al for oxygen, high oxygen incorporation is another source for the defects in the AlN films. From the previous observation, high discharge power can induce high stress in the AlN films. As the power increases, the effects of resputtering, input of heat into the surface and increasing surface mobility of depositing generation of point defects are increasingly pronounced. Moreover, the defects, together with resputtering, also cause destruction of the columnar growth morphologies and a large enhancement in the stress of the films. These defects undoubtedly cause the intrinsic stresses in the AlN films. Furthermore, the adatom mobility is enhanced at high power, owing to the increase in the kinetic energy transfer from the bombarding particles, and thus the deposited temperature is also increased. Since the thermal strain in AlN film deposited at higher temperature is given by ($\alpha_{\mathrm{AlN}}-\alpha_{\mathrm{Si}}$) ΔT (α, the thermal expansion coefficient, ΔT the difference between deposition temperature and room temperature), the AlN films deposited at higher discharge power have larger thermal stress. Accordingly, the film strain for both Si (100) and Si (111) substrates increased with the increasing of discharge power, as shown in Fig. 4. However, it can also found from Fig. 4 that the strain increase largely with discharge power for Si (111), and it does not change so obviously for Si (100). The strain difference in the AlN films deposited on the two types of the substrates can be attributed to the extent of lattice mismatch. If we consider AlN stacking in the Si substrate, the coincident sites can be found by the superposition of the two Si and AlN lattice to form a bicrystal. If the two lattices are commensurate, the interfacial structure is strictly periodic, and a new coincidence lattice can be built. If incommensurate, the closest fractional approximation defines a quasicoincident lattice which is valid, at least locally. The XRD spectra in Fig. 1 have proved that the preferred (0002) orientation of AlN film can be attained. The lattices in AlN (0001) and Si (111) both exhibit hexagonal, and thus Si (111) plane can provide a matched template for AlN (0001) plane. The lattice mismatch between these two plane is 19% ($d_{\mathrm{Si}\ (111)}-d_{\mathrm{AlN}\ (0001)}/d_{\mathrm{Si}\ (111)}$, here $d_{\mathrm{Si}\ (111)}$ refers to the Si lattice distance in Si (111) plane; $d_{\mathrm{AlN}\ (0001)}$ refers to the AlN lattice distance in AlN (0001) plane). The lattice in Si (100) is square, which is unmatched with hexagonal lattice in AlN (0001) plane. The lattice mismatch between AlN (0001) and Si (100) is 42.7% ($d_{\mathrm{Si}\ (100)}-d_{\mathrm{AlN}\ (0001)}/d_{\mathrm{Si}\ (100)}$, here, $d_{\mathrm{Si}\ (100)}$ refers to the Si lattice distance in Si (100) plane). The larger lattice mismatch between AlN (0001) and Si (100) is a main contribution to the larger strain in the formed films, and therefore the discharge power does not influence the strain in AlN films deposited on Si (100) obviously. For Si (111) substrates, the lattice mismatch between the film and substrate is smaller, and the strain due to defects and thermal mismatch contributes largely to the residual strain in the deposited films. Thus, the strain in the films deposited on Si (111) largely depends on the discharge power in sputtering.

4. Conclusions

Highly oriented AlN thin films as buffer layer in GaN growth can be fabricated by RF reactive magnetron sputtering. Through studying the crystallographic orientation and the strain in the films deposited by different discharge power, it is found that the orientation of the silicon substrates can influence greatly the strain in the deposited films. For Si (100) substrates, the large lattice mismatch between AlN (0001) and Si (100) is a main contribution to the large strain in the formed films, and the strain does not change too much with discharge power. For Si (111) substrates, the strain increases obviously with discharge power, and the strain part introduced by defects and thermal mismatch is a main contribution to the residual strain in the films.

References

[1] B. Gil, Group III Nitride Semiconductor Compounds: Physics and Application, Clarendon, Oxford, 1998.
[2] V. Lebedev, J. Jinschek, U. Kaiser, B. Schroter, W. Richter, J. Kraublich, Appl. Phys. Lett. 76 (2000) 2029.
[3] I. Akasaki, H. Amano, Y. Koide, K. Hiramatsu, N. Sawaki, J. Cryst. Growth 98 (1989) 209.
[4] K. Hiramatsu, S. Itoh, H. Amano, I. Akasaki, N. Kuwano, T. Shiraishi, K. Oki, J. Cryst. Growth 115 (1991) 628.
[5] S. Nakamura, Jpn. J. Appl. Phys. 30 (1991) 1620.
[6] X.D. Wang, W. Jiang, M.G. Norton, K.W. Hipps, Thin Solid Films 251 (1994) 121.

[7] H. Morkoc, Nitride Semiconductors and Devices, Springer, New York, 1999.
[8] H. Amano, N. Sawaki, I. Akasaki, Y. Toyoda, Appl. Phys. Lett. 48 (1986) 353.
[9] J. Keckes, G. Koblmueller, R. Averbeck, J. Cryst. Growth 246 (2002) 73.
[10] T. Lei, M. Fanciulli, R.J. Molnar, T.D. Moustakas, R.J. Graham, J. Scanlon, Appl. Phys. Lett. 59 (1991) 944.
[11] Y. Lu, X.L. Liu, D.C. Lu, H.R. Yuan, G.Q. Hu, X.H. Wong, Z.G. Wang, X.F. Duan, J. Cryst. Growth 247 (2003) 91.
[12] J.R. Gong, M.F. Yeh, C.L. Wang, J. Cryst. Growth 247 (2003) 261.
[13] T. Paskova, E. Valcheva, J. Birch, S. Tungasmita, P.-O.A. Persson, P.P. Paskov, S. Evtimova, M. Abrashev, B. Monemar, J. Cryst. Growth 230 (2001) 381.
[14] J. Wan, R. Venngopal, M.R. Melloch, H.M. Liaw, W.J. Rummel, Appl. Phys. Lett. 79 (2001) 1459.
[15] W.J. Meng, J.A. Sell, T.A. Perry, L.E. Rehn, P.M. Baldo, J. Appl. Phys. 75 (1994) 3446.
[16] W.J. Meng, J.A. Sell, T.A. Perry, J. Appl. Phys. 74 (1993) 2411.
[17] A. Bourret, A. Barski, J.L. Rouviere, G. Renaud, A. Barbier, J. Appl. Phys. 83 (1998) 2003.
[18] X.H. Xu, H.S. Wu, C.J. Zhang, Z.H. Jin, Thin Solid Films 388 (2001) 62.
[19] B.D. Cullity, S.R. Stock, Elements of X-Ray Diffraction, 3rd ed., Prentice Hall, 2001.
[20] T. Prokofyeva, M. Seon, J. Vanbuskirk, M. Holtz, Phys. Rev., B 63 (2001) 125313.
[21] Y.F. Lu, Z.M. Ren, T.C. Chong, B.A. Cheong, S.K. Chow, J.P. Wang, J. Appl. Phys. 87 (2000) 1540.
[22] K. Jagannadham, A.K. Sharma, Q. Wei, R. Kalyanraman, J. Narayan, J. Vac. Sci. Technol., A, Vac. Surf. Films 16 (1998) 2804.
[23] J.H. Edgar, C.A. Carosella, C.R. Eddy Jr., D.T. Smith, J. Mater. Sci., Mater. Electron. 7 (1996) 247.
[24] S. Oktyabrsky, K. Dovidenko, A.K. Sharma, V. Joshkin, J. Narayan, MRS Internet J. Nitride Semicond. Res. 4S1 (1991) 43.